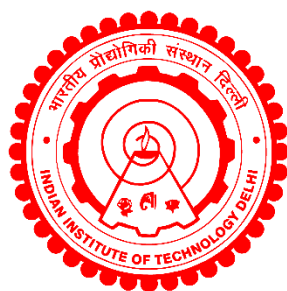


**MOLECULAR INSIGHTS AND THERAPEUTIC POTENTIAL
OF NATURAL COMPOUNDS**

VIPUL KUMAR



**DEPARTMENT OF BIOCHEMICAL ENGINEERING AND BIOTECHNOLOGY
INDIAN INSTITUTE OF TECHNOLOGY DELHI**

JULY 2023

© Indian Institute of Technology Delhi (IITD), New Delhi, 2023

MOLECULAR INSIGHTS AND THERAPEUTIC POTENTIAL OF NATURAL COMPOUNDS

by

Vipul Kumar

Department of Biochemical Engineering and Biotechnology

Submitted

*in the fulfilment of the requirements of the degree of Doctor of Philosophy
to the*



Indian Institute of Technology Delhi

JULY 2023

CERTIFICATE

This is to certify that the thesis entitled '**Molecular insights and therapeutic potential of natural compounds**' being submitted by Mr. Vipul Kumar to the Indian Institute of Technology Delhi for the award of the degree of '**Doctor of Philosophy**', is a record of the bonafide research work carried out by him, which has been prepared under my supervision in conformity with the rules and regulations of Indian Institute of Technology Delhi. The research reports and the results presented in the thesis have not been submitted for any degree or diploma in any other University or Institute.

Prof. D. Sundar

Institute Chair Professor

Department of Biochemical Engineering and Biotechnology

Indian Institute of Technology Delhi

ACKNOWLEDGEMENTS

I would like to express my sincere gratitude to my supervisor Prof. D. Sundar for his constant support and encouragement throughout my PhD journey. His invaluable guidance has been instrumental in helping me with my work and the writing of this thesis. I could not have asked for a better advisor and mentor for my Ph.D. study. I am truly grateful for all that he has done for me. I would also like to thank Dr. Renu Wadhwa and Dr. Sunil Kaul from AIST, Japan, for the wet lab experiments and their valuable advice.

I sincerely thank my thesis committee, Prof. Ravikrishnan Elangovan, Prof. Preeti Srivastava, and Prof. Ashok Patel (Kusuma School of Biological Sciences at IITD), for their insightful comments, encouragement and the questions that have motivated me to broaden my research from various perspectives.

I would like to express my gratitude to my fellow lab-mates for their stimulating discussions, the work we did together, and the fun we had in the last few years. I especially want to thank Dr. Jaspreet Kaur Dhanjal for her help, guidance, support, and always being there for me throughout my PhD journey. Additionally, I would like to thank Dr. Vidhi Malik for the guidance and support. I would also like to thank Mr. Yogesh Kalakoti, Dr. Dhvani Vora, Mr. R. Navaneethan, Mr. Seyad Shefrin, Ms. Pragya Keshwarwani, Ms. Swathik Calaranica, Mr. Kamlesh Kumar, Mr. Inam Ahmed, and everyone who has shared the lab with me at some point during this long journey, for always being helpful and keeping the lab environment cheerful and enjoyable. Furthermore, I would also like to express my gratitude and appreciation to my batchmates and friends, particularly Yogesh, Garima, Praveen, Abhijeet, Aditi and Sakshi. Thanks for making this journey so much fun.

I would like to extend my deepest gratitude to my parents for their constant love, encouragement, and unwavering support throughout my academic journey. Their sacrifices, guidance, and belief in me have been the foundation of my success, and I am forever grateful. I also want to thank Vibhav and Rupam for their love, support, and understanding. Thank you all from the bottom of my heart.

Vipul Kumar

ABSTRACT

The high cost of drugs and the speed of growing drug resistance has made modern medicine unaffordable to people in economically impoverished and developing countries. However, traditional home remedies are often cheaper and have fewer side effects but are not always accepted because of a lack of scientific understanding. Therefore, the goal of this thesis was to investigate the molecular mechanisms of compounds found in natural sources using computational simulations supplemented with experimental evidence. Withanolides derived from the Ashwagandha plant and compounds from the honeybee propolis are the main focus of this thesis. Firstly these natural compounds were investigated against cancer-related targets. Withaferin-A (Wi-A) and Withanone (Wi-N) from Ashwagandha and Caffeic Acid Phenethyl Ester (CAPE) from honeybee propolis were found to be potent against DNA methyltransferases. The studies suggested that Withanolides might also be potent against Phosphodiesterase-4D (PDE4D) related cancers. Furthermore, the antiviral properties of the natural compounds were studied. Withanolides such as Withanone-IV, Withanoside-V and Withanone and honeybee propolis-related compounds such as CAPE, individually and in combination were effective against Severe Acute Respiratory Syndrome Coronavirus 2 (SARS-CoV-2) *in silico* and *in vitro* experiments. Additionally, natural products were explored to investigate their ability to overcome cancer resistance by inhibiting efflux proteins such as ATP-binding cassette subfamily G member 2 (ABCG2). The study suggested that Stock1n-87939 (3-(5,11-dioxoisindolo[2,1-a]quinazolin-6(5H,6aH,11H)-yl)-N-(1H-indol-4yl)propanamide) could be a potent ABCG2 inhibitor. Ashwagandha and honeybee propolis compounds have been shown to have neuroprotective effects in the literature. However, no experimental evidence was present on whether they could penetrate the Blood Brain Barrier (BBB). Hence, steered molecular dynamics simulation and the umbrella sampling approach were used to study the passive diffusion of the natural compounds through BBB. It was found that only CAPE, but not the Withanolides (Wi-A and Wi-N), was found to be permeable through BBB and hence could be used as potential neurotherapeutics.

Overall, the thesis presents compelling evidence supporting the potential of natural products as a valuable source for drug discovery. The implications of these findings could pave the way for the development of safer and more effective drugs.

सार

दवाओं की उच्च लागत और बढ़ती दवा प्रतिरोध की गति ने आर्थिक रूप से गरीब और विकासशील देशों में आधुनिक चिकित्सा को लोगों के लिए अवहनीय बना दिया है। हालाँकि, पारंपरिक घरेलू उपचार अक्सर सस्ते होते हैं और इनके कम दुष्प्रभाव होते हैं लेकिन वैज्ञानिक समझ की कमी के कारण इन्हें हमेशा स्वीकार नहीं किया जाता है। इसलिए, इस शोध प्रबंध का लक्ष्य प्रायोगिक साक्ष्य के साथ पूरक कम्प्यूटेशनल सिमुलेशन का उपयोग करके प्राकृतिक स्रोतों में पाए जाने वाले यौगिकों के आणविक तंत्र की जांच करना है। अश्वगंधा पौधे से प्राप्त विथेनोलाइड्स और हनीबी प्रोपोलिस से यौगिक इस शोध प्रबंध के मुख्य केंद्र हैं। सबसे पहले इन प्राकृतिक यौगिकों की जांच कैंसर संबंधी लक्ष्यों के विरुद्ध की गई। अश्वगंधा से विथाफेरिन-ए (Wi-A) और विथेनोन (Wi-N) और हनीबी प्रोपोलिस से कैफिक एसिड फेनिथाइल एस्टर (CAPE) डीएनए मिथाइलट्रांसफेरेज़ के खिलाफ शक्तिशाली पाए गए। हमारे अध्ययनों ने सुझाव दिया कि विथेनोलाइड्स फॉस्फोडिएस्टरेज़-4डी (पीडीई4डी) से संबंधित कैंसर के खिलाफ भी शक्तिशाली हो सकते हैं। इसके अलावा, हमने प्राकृतिक यौगिकों के एंटीवायरल गुणों पर ध्यान दिया। Withanone-IV, Withanoside-V और Withanone जैसे Withanolides और CAPE जैसे हनीबी प्रोपोलिस-संबंधित यौगिक, व्यक्तिगत रूप से और संयोजन में, सिलिको और इन विट्रो प्रयोगों में गंभीर एक्वूट एक्वूट रेस्पिरेटरी सिंड्रोम कोरोनावायरस 2 (SARS-CoV-2) के खिलाफ प्रभावी हैं। इसके अतिरिक्त, एटीपी-बाइंडिंग कैसेट सबफैमिली जी मेंबर 2 (एबीसीजी2) जैसे एफ्लक्स प्रोटीन को बाधित करके कैंसर प्रतिरोध को दूर करने की उनकी क्षमता की जांच करने के लिए प्राकृतिक उत्पादों का पता लगाया गया है। अध्ययन ने सुझाव दिया कि Stock1n-87939 (3-(5,11-डाइऑक्सोइसोइंडोलो[2,1-a]quinazolin-6(5H,6aH,11H)-yl)-N-(1H-indol-4yl)propanamide) हो सकता है एक शक्तिशाली ABCG2 अवरोधक। अश्वगंधा और हनीबी प्रोपोलिस यौगिकों को साहित्य में न्यूरोप्रोटेक्टिव प्रभाव दिखाया गया है। हालांकि, इस बात का कोई प्रायोगिक साक्ष्य मौजूद नहीं था कि वे ब्लड ब्रेन बैरियर (बीबीबी) में प्रवेश कर सकते हैं या नहीं। इसलिए, बीबीबी के माध्यम से प्राकृतिक यौगिकों के निष्क्रिय प्रसार का अध्ययन करने के लिए स्टीयर आणविक गतिशीलता सिमुलेशन और छाता नमूनाकरण दृष्टिकोण का उपयोग किया गया था। यह पाया गया कि केवल CAPE, लेकिन Withanolides (Wi-A और Wi-N) नहीं, BBB के माध्यम से पारगम्य पाया गया और इसलिए इसे संभावित न्यूरोथेरेप्यूटिक्स के रूप में इस्तेमाल किया जा सकता है।

कुल मिलाकर, शोध प्रबंध दवा की खोज के लिए एक मूल्यवान स्रोत के रूप में प्राकृतिक उत्पादों की क्षमता का समर्थन करने वाले सम्मोहक साक्ष्य प्रस्तुत करती है। इन निष्कर्षों के निहितार्थ सुरक्षित और अधिक प्रभावी दवाओं के विकास का मार्ग प्रशस्त कर सकते हैं।

CONTENTS

Certificate	i
Acknowledgements	ii
Abstract	iii
Contents	v
List of Figures	x
List of Tables	xv
List of Equations	xvi
List of Abbreviations	xvii
1 Introduction	1
1.1 Natural products as traditional medicine and their use in modern drug discovery.....	1
1.2 Reports on the therapeutic potential of Ashwagandha and honeybee propolis-derived ingredients.....	3
1.3 The computational approaches used in drug discovery and probing the molecular interactions	5
1.4 Motivation for the thesis.....	13
1.5 Definition of the problem.....	13
1.6 Objectives of the thesis.....	14
1.7 Thesis organization.....	14
2 The anti-cancer potential of ashwagandha and honeybee propolis-derived compounds	18
2.1 Introduction	18
2.2 Effect of Withaferin-A, Withanone and Caffeic Acid Phenethyl Ester on DNA methyltransferases: potential in epigenetic cancer therapy	19
2.2.1 Background	19
2.2.2 Methods	21
2.2.2.1 Preparation of molecular structures and molecular docking	21

2.2.2.2 MD simulations of the docked complexes and trajectory analysis	22
2.2.3 Results and Discussion.....	23
2.2.3.1 SFG and Wi-A have a similar binding affinity towards DNMT1 and DNMT3A, while CAPE against DNMT3A.....	23
2.2.3.2 Natural compounds treated cells showed upregulation of p16 ^{INK4A} expression	29
2.2.4 Conclusion.....	30
2.3 Computational insights into the potential of Withanolides as Phosphodiesterase (PDE4D) inhibitor.....	30
2.3.1 Background	30
2.3.2 Methods.....	32
2.3.2.1 Ligand retrieval, filtering, and inverse virtual screening.....	32
2.3.2.2 Preparation of the protein-ligand complexes and molecular docking	32
2.3.2.3 MD simulations and analysis of the trajectories.....	33
2.3.3 Results	34
2.3.3.1 Ligand-based inverse virtual screening predicts protein kinase C isoforms, AR, PTGS-2 and PDE4D as therapeutic targets of Withanolides	34
2.3.3.2 Structure-based study shows the inhibitory potential of Withanolides against PDE4D.....	38
2.3.4 Conclusion.....	43
2.4 Overall summary of the chapter	43
3 Computational and experimental evidence of the anti-COVID-19 potential of Ashwagandha and Honeybee propolis-derived natural compounds.....	44
3.1 Introduction	44
3.2 The mechanistic insights into the interactions and energetics of the Alpha, Kappa and Delta variants of Spike protein with hACE2 receptor.....	45
3.2.1 Background	45

3.2.2	Methods	47
3.2.2.1	Preparation of the mutants and MD simulation	47
3.2.2.2	Analysis of the MD simulation	48
3.2.3	Results and Discussion	49
3.2.3.1	Mutants showed higher affinity and increased stability than Wildtype	49
3.2.4	Conclusion	54
3.3	The binding mechanism and inhibitory potential of Withanolides and honeybee propolis-related compounds against TMPRSS2	55
3.3.1	Background	55
3.3.2	Methods	57
3.3.2.1	Retrieval of the structures and their preparation for molecular simulations	57
3.3.2.2	Grid generation and molecular docking	58
3.3.2.3	The MD simulation and trajectory analysis	58
3.3.3	Results and Discussion	58
3.3.3.1	The binding affinity of Withanolides towards TMPRSS2 predicted Withanoside-V and Withanoside-IV as the best among all the Withanolides	58
3.3.3.2	ARC and Cyclodextrins but not CAPE, showed stable binding at the active site of TMPRSS2	64
3.3.4	Conclusion	67
3.4	The mechanism of the binding against the M^{pro} and antiviral potential of the natural compounds against SARS-CoV-2	67
3.4.1	Background	67
3.4.2	Methods	68
3.4.3	Results and Discussion	69
3.4.3.1	The binding affinity of Withanolides towards SARS-CoV-2 Main protease (M ^{pro}) predicted Withanoside-V as the best among all the Withanolides	69

3.4.3.2 Selected Withanolides and propolis compounds caused inhibition of SARS-CoV-2 replication	74
3.4.4 Conclusion.....	75
3.5 Overall summary of the chapter	76
4 The potential of natural compounds to enhance the bioavailability of therapeutic drugs and their membrane permeability	77
4.1 Introduction	77
4.2 Structure-based discovery of novel ABCG2 natural product inhibitors: A high throughput virtual screening and molecular dynamics study.....	78
4.2.1 Background	78
4.2.2 Methods.....	80
4.2.2.1 Protein structure retrieval, preparation and grid generation for molecular docking and simulation.....	80
4.2.2.2 Redocking of Tariquidar and virtual screening workflow to screen natural products	80
4.2.2.3 Explicit water MD simulations and their analysis.....	81
4.2.3 Results and Discussion.....	82
4.2.3.1 Virtual screening of 69067 compounds from the IBS screen database suggested Stock1n-4065, Stock1n-87939 and Stock1n-89084 as the top-hit compounds	82
4.2.3.2 MD study predicted Stock1n-87939 could be the lead compound for the inhibition of ABCG2	85
4.2.4 Conclusion.....	89
4.3 All-atom molecular dynamics-based study of permeability of natural compounds through Blood Brain Barrier Lipid Model	90
4.3.1 Background	90
4.3.2 Methods.....	92
4.3.2.1 Modelling of BBB lipid bilayer.....	92

4.3.2.2	Minimization and equilibration of the lipid bilayer system	92
4.3.2.3	Properties of the lipid bilayer	93
4.3.2.4	Free energy calculations	93
4.3.2.5	The diffusion and the permeability of the small molecules.....	94
4.3.3	Results and Discussion.....	95
4.3.3.1	The prepared BBB model properties were consistent with experimental data.....	96
4.3.3.2	Diffusion, PMF and Resistivity profiles of the small molecules.....	97
4.3.3.3	CAPE was found to be the most permeable among the studied natural compound	99
4.3.4	Conclusion.....	101
4.4	Overall summary of the chapter	101
5	Conclusion of the Thesis	102
6	References	105
7	Appendices	127
8	List of publications	137
9	Resume of the author	139

LIST OF FIGURES

- Figure 1-1. Natural compounds studied for their anticancer activities.** (A) Withaferin-A (Wi-A) and (B) Withanone (Wi-N); the steroidal lactones derived from Ashwagandha plant (C) Caffeic Acid Penethyl Ester (CAPE) and (D) Artepillin-C (ARC); phenolic compounds from honeybee propolis. 4
- Figure 1-2. The approaches and methods used in computational drug discovery.** (A) The Computer-aided drug discovery (CADD) process can have multiple approaches depending on the therapeutic target and drug molecule information. (B) The Structure-Based Drug Discovery (SBDD) shows virtual screening methods and molecular dynamics (MD) simulation. (HTS: High Throughput Screening; ADME: Absorption Distribution Metabolism Excretion; HTVS: High Throughput Virtual Screening). 6
- Figure 1-3. The process of Molecular dynamics simulations.** In classical MD simulations, Newtonian mechanics is applied to move the molecules from their initial position based on the natural interacting forces acting on them. However, the steered MD and Umbrella sampling uses the additional biased potential (natural plus biased forces taken as total force, and it is integrated for movement of molecules) to pull and restrict the molecules, respectively. After sampling each window, the weighted histogram analysis method (WHAM) algorithm is then used to calculate the potential of mean force (PMF) throughout the coordinate. 10
- Figure 2-1. The catalytic site residues of DNA Methyltransferases (DNMT1 and DNMT3A) interacting with ligands in the best-docked pose.** (A) DNMT1/SFG (B) DNMT1/CAPE (C) DNMT1/Wi-A (D) DNMT1/Wi-N (E) DNMT3A/SFG (F) DNMT3A/CAPE (G) DNMT3A/Wi-A (H) DNMT3A/Wi-N. (SFG: Sinefungin)..... 24
- Figure 2-2. The MD simulation of DNMTs with natural compounds** (A) The RMSD plot showing the stable trajectory of DNMTs/ligand complex (A) DNMT1 (B) DNMT3A (C) The RMSF plot showing the flexibility/fluctuation of the DNMT1 residues, the loop region (1100-1110) had the highest fluctuation. (D) RMSF of the amino acid residues of DNMT3A. Fluctuations were observed in the catalytic region between 835-850 of the protein. (E) The MM/GBSA free binding energy of the DNMT1/ligand complexes, showing the Wi-A had identical binding as SFG towards DNMT1 (F) The MM/GBSA free binding energy of the DNMT1/ligand complexes..... 25
- Figure 2-3. Polar and non-polar interactions occupancy of various critical residues of DNMT1 and DNMT3A during the simulation run in case of binding with** (A) DNMT1/SFG, (B) DNMT1/CAPE, (C) DNMT1/Wi-A (D) DNMT1/Wi-N (E) DNMT3A/SFG (F) DNMT3A/CAPE (G) DNMT3A/Wi-A and (H) DNMT3A/Wi-N.(Blue color: water bridge interactions; Violet color: hydrophobic interactions; Green color: hydrogen bonds) 27
- Figure 2-4. Determination of toxicity and effect of treatment of natural compounds on tumor suppressor protein.** (A) The nontoxic doses Wi-A, Wi-N and CAPE. (B) An increase in p16INK4A was detected at the protein level treated with Wi-A, Wi-N and CAPE..... 29
- Figure 2-5. The Plant-Compounds-Targets network shows the top predicted targets for the Withanolides from Ashwagandha.** The bigger target node indicated more number of interactions. The top 6 targets, namely, Protein kinase C alpha (PRKCA), Protein kinase C delta (PRKCD), Protein kinase C epsilon

(PRKCE), Androgenic Receptor (AR), Cyclooxygenase-2 (PTGS-2) and Phosphodiesterase-4D (PDE4D), had more than 15 node interactions with the Withanolides.....	36
Figure 2-6. The best-docked pose of ligands with PRKCE (A) Sotrastaurin (B) 27-HydroxyWithanolide-B (C) Withanolide-P (D) Withanolide-E (E) The number of hydrogen bonds throughout the simulations and (F) MM/GBSA of Sotrastaurin was too high in comparison with the Withanolides	37
Figure 2-7. The best-docked pose of Zardaverine with PDE4D, making two hydrogen bonds with Asn418 and Gln466.	38
Figure 2-8. The best-docked pose of the ligands and their hydrogen bond interactions with PDE4D. (A) 17-Hydroxywithaferin-A, (B) 27-Hydroxywithanone, (C) Withanolide-R, (D) Withaferin-A.....	39
Figure 2-9. The kernel density plot showing the variation in the dynamics of the complexes in the two main principal components. Overall, no similarity was found among the dynamics of the complexes, but when positive control complex (PDE4D-Zardaverine) was superimposed on the representative structure of the clusters of PDE4D-Withanolide-R, PDE4D-17-Hydroxywithaferin-A, 27-Hydroxywithanone and Withaferin-A, it was found that the structural change was small.....	40
Figure 2-10. The MD simulation analysis of PDE4D-ligand complexes (A) The RMSD plot showing the stable trajectory of the protein-liagnd complexes (B) No significant fluctuation seen in the RMSF (C) The average number of hydrogen bonds shows that the Zardaverine, 17-Hydroxywithaferin-A and 27-Hydroxywithanone had more than one average hydrogen bonding throughout the simulations. (D) The MM/GBSA binding energy shows that Withanolide-R had the best binding affinity towards PDE4D, while all other ligands had similar binding energy.	41
Figure 2-11. The simulation interaction diagram shows the fraction of the interactions between the PDE4D and the potential inhibitors throughout the 100ns of MD simulations. (A) Zardaverine (B) Withanolide-R (C) Withaferin-A (D) 17-Hydroxywithaferin-A (E) 27-Hydroxywithanone.....	42
Figure 3-1. The Receptor Binding Domain (RBD) structure of SARS-CoV-2 Spike protein complexed with human Angiotensin Converting Enzyme 2 (hACE2) receptor. (A) The sphere shape residues in hot pink colour show N501Y mutation in Spike protein of SARS-CoV-2. (B) at L452R, T478K and E484Q mutation in the Spike protein (RBD) of B.1.617 lineage.	46
Figure 3-2. MD simulation analysis of the three simulated complexes. (A) RMSD plot showing similar deviation of all the simulated structures. (B) RMSF plot reveals that Residues 350-400 of the spike receptor binding domain (RBD) are more flexible, while the mutated residues have lesser fluctuation and are comparable in all three structures. (C) The number of hydrogen bond counts indicates that WT and Kappa variants have similar and higher hydrogen bonds than Delta and Alpha. (D) MM/GBSA binding free energy of the 20 structure complexes extracted from each trajectory at equal span, suggesting that Kappa and Alpha spike variants have a higher affinity for hACE2 than Delta and WT.....	50
Figure 3-3. The fraction of hydrogen bonds between Spike and hACE2 of different variants. (A) The hydrogen bond occupancy in WT spike-hACE2 complex (B) Alpha variant (C) Kappa and (D) Delta variant throughout the 200ns of MD simulations.....	51
Figure 3-4. Comparing the interaction of the mutated and wild-type residues in the three structures extracted at 50ns span from the simulated trajectories: Spike protein (blue color), hACE2 (orange color). (A) The Kappa spike variant and their interactions; GLN484 of Spike protein makes the intra-chain	

hydrogen bond with SER349 and ASN450 in the 100th and 150th ns frame. (B) Alpha Spike variant interactions; The hydrogen bond interaction of TYR501 of mutant Spike protein with LYS353 of hACE2 in the 100th and 150th ns frame (C) The interaction of wild type residues at 50th, 100th and 150th ns of the simulation shows that GLU484 of spike protein had only one hydrogen bond interaction with SER349 or TYR351 of Spike itself. Similarly, ASN501 of Spike only made hydrogen bond interaction with its residues. (D) In the Delta Spike variant, at the 100th ns frame, the addition of hydrogen bond of LYS478 with SER476 was observed. 52

Figure 3-5. Chemical structure of the natural compounds studied. Camostat mesylate, Withanoside-V, Methoxy Withaferin A, Withanolide-A, Withaferin-A, Withanolide-B, 12-deoxywithastramonolide, Withanoside-IV, Withanone, Cyldoextrins, CAPE and ARC. 57

Figure 3-6. The best docked pose of Camostat mesylate with TMPRSS2. 58

Figure 3-7. Interactions of TMPRSS2 residues with the ligands in the best-docked pose. (A) TMPRSS2-Withanolide-A (B) TMPRSS2-Withanoside-V (C) TMPRSS2-Withanoside-IV (D) TMPRSS2-Methoxy Withaferin-A (E) TMPRSS2-Withanolide-B (F) TMPRSS2-Withaferin-A (G) TMPRSS2-Withanone (H) TMPRSS2-12-deoxywithastramonolide. 59

Figure 3-8. The analysis of the Molecular Dynamics (MD) simulations of TMPRSS2 with Camostat mesylate and other Ashwagandha derived compounds. (A) The stable RMSD trajectory of ligands when bound to TMPRSS2. (B) RMSD of protein-ligand complexes showing a stable trajectory without any significant deviations. (B) The RMSF of the amino acid residues of the protein when bound with different ligands, fluctuations were observed only in the outer loop region, Pro335 to Lys340 of the TMPRSS2. protease. 61

Figure 3-9. Effect of different Withanolides on TMPRSS2 mRNA levels in T.Tn cells 64

Figure 3-10. The interaction of the natural molecules from propolis with TMPRSS2. (A)Alpha-Cyclodextrin (B) Artepillin-C (C) Caffeic Acid Phenethyl Ester (CAPE) (D) Beta-Cyclodextrin (E) Gamma-Cyclodextrin (F) The RMSD plot showing the stable interaction of the TMPRSS2 complexed with the ligands throughout the simulation time. 65

Figure 3-11. The simulation interaction fraction of TMPRSS2 with propolis compounds. (A) Artepillin-C (B) Alpha-cyclodextrin (C) Gamma-cyclodextrin. 66

Figure 3-12. The interaction of N3 inhibitor with M^{pro} in the best docking pose. 69

Figure 3-13. Interactions of M^{pro} residues with the ligands in the best-docked pose. (A) M^{pro}- Withanoside-IV (B) M^{pro}-Withanoside-V (C) M^{pro}-Withanolide-A (D) M^{pro}-Methoxy Withaferin-A (E) M^{pro}-12-deoxywithastramonolide (F) M^{pro}-Withaferin-A (G) M^{pro}-Withanolide-B (H) M^{pro}- Withanone. 70

Figure 3-14. The analysis of the MD simulation trajectories of M^{pro} with different ligands. (A) RMSD of the ligands when bound to M^{pro}. (B) RMSD of the M^{pro}-ligand complexes showing a stable trajectory without any significant fluctuation. (C) RMSF of the amino acid residues of the M^{pro} when bound with ligands. . 72

Figure 3-15. Anti-viral activity of Wi-A, CAPE and Wi-ACAPE. Quantitation of the staining shows viability (blue) and virus inhibition (red). 75

Figure 4-1. ABCG2 structure. (A) The structure of ABCG2 homodimer with two cavities, cavity1, the substrate/inhibitor binding site, cavity2, from where substrates are released into the cytoplasm. Plug

(Leu554) separates cavity1 from cavity2. (B) The different Transmembrane helices, The TMD interface is formed by TM2 and TM5a of opposing ABCG2 monomers.	79
Figure 4-2. The best-docked pose of ligands shows the polar contacts and docking score with ABCG2. (A) Tariquidar (B) Stock1n-43065 (C) Stock1n-87939 (D) Mitoxantrone (E) Stock1n-89084.	84
Figure 4-3. The 2D image of the top screened natural compounds. (A) Stock1n-43065 (B) Stock1n-87939 (C) Stock1n-89084.	84
Figure 4-4. The analysis of the MD simulation trajectories of ABCG2-ligand complexes. (A) The RMSD plot shows the systems got stabilized within 40 ns of simulation. (B) The RMSF plot shows the fluctuation in the individual amino acids; significantly less fluctuation is observed in the ligand-binding residues. (C) The number of hydrogen bonds forming between ligands and ABCG2 throughout the simulation. (D) The MM/GBSA binding free energy of 50 frames extracted from 100-200ns of simulation data indicates the highest binding affinity of Stock1n-87939 with ABCG2.	86
Figure 4-5. The different kinds of interactions and the interaction fractions of ABCG2 with ligands throughout the simulation. (A) Tariquidar (B) Mitoxantrone (C) Stock1n-43065 (D) Stock1n-89084 (E) Stock1n-89084.	87
Figure 4-6. The 2D images of the small molecules studied. (A) Antipyrine (B) Ibuprofen (C) Mannitol (D) CAPE (E) Wi-N (F) ARC (G) Wi-A.	91
Figure 4-7. The 3D representation of the modelled BBB bilayer model. The equilibrated model contains POPC in red, POPE in orange, PSM in grey, cholesterol in yellow, and SSM in green.	95
Figure 4-8. The structural properties of lipid molecules. (A) The density profile of all the molecules within the system shows the distribution of their localization (0 represents the centre of the bilayer). (B) The average area per lipid profile of the lipid molecules. (C, D) The Sn1 and Sn2 order parameters of the lipid molecules in the BBB model.	97
Figure 4-9. The Diffusion and PMF profile of small molecules. (A) The diffusion profile shows the higher diffusion of smaller molecules and a higher diffusion rate in the water. (B) The PMF profile shows the highest energy barrier of Wi-A and Wi-N and the lowest for CAPE to pass the BBB.	98
Figure 4-10. The resistivity profile of the small molecules. (A) Antipyrine (B) Mannitol (C) Mannitol (C) Wi-A(D) Wi-N (E) ARC (F) Ibuprofen (G) CAPE.	99

LIST OF TABLES

Table 1-1. The approved bioactive molecules derived from natural products have therapeutic potential...	2
Table 2-1. The analysis of MD simulation trajectories of PDE4D with natural compounds.	40
Table 3-1 The residue-wise energy contribution of the mutated residues compared with the wildtype for the twenty structures extracted from 50 to 200 ns of the simulation for all three complexes.	53
Table 3-2. TMPRSS2 residues interacting with the ligands in their best-docked pose.	60
Table 3-3. Residues of TMPRSS2 interacting with the ligands during the course of MD simulations along with the free binding energy of each protein-ligand complex. The significant interactive residues have been shown in bold.	63
Table 3-4. M^{pro} residues interacting with the ligands in their best-docked pose.	71
Table 3-5. Residues of M^{pro} interacting with the ligands during the course of MD simulations, along with the free binding energy of each protein-ligand complex.	73
Table 3-6. Inhibition of SARS-CoV-2 replication by Withanolides.	74
Table 4-1. The top 10 compounds screened through virtual screening workflow against ABCG2.	83
Table 4-2. The distribution of different lipid molecules in the BBB model	92
Table 4-3 The LogP and BBB prediction of the tested small molecules.	100

LIST OF EQUATIONS

Equation 1-1	8
Equation 1-2	8
Equation 1-3	8
Equation 1-4	9
Equation 1-5	9
Equation 1-6	9
Equation 1-7	9
Equation 1-8	11
Equation 1-9	12
Equation 1-10	12
Equation 1-11	12
Equation 2-1	23
Equation 2-2	23
Equation 2-3	23
Equation 2-4	23
Equation 4-1	93

LIST OF ABBREVIATIONS

ACE2	Angiotensin-converting enzyme 2
ABCG2	ATP-binding cassette subfamily G member 2
ARC	Artepillin C
ADME	Absorption Distribution Metabolism Excretion
BBB	Blood Brain Barrier
CADD	Computer-Aided Drug Discovery
CAPE	Caffeic Acid Phenethyl Ester
COVID-19	CoronaVirus Disease
DNMTs	DNA Methyl Transferases
HIF	Hypoxia Inducible Factor
HTS	HighThroughput Screening
HTVS	HighThroughput Virtual Screening
LBDD	Ligand-Based Drug Discovery
MM	Molecular Mechanics
MMGBSA	Molecular Mechanics Generalised Born and Surface Area
M ^{pro}	Main Protease
POPC	Phosphatidylcholine
POPE	Phosphatidylethanolamine
PDE4D	Phosphodiesterase 4D
QSAR	Quantitative Structure-Activity Relationship
RMSD	Root Mean Square Deviation
RMSF	Root Mean Square Fluctuation
SARS-CoV-2	Severe Acute Respiratory Syndrome-CoronaVirus 2
SBDD	Structure-Based Drug Discovery
SMD	Steered Molecular Dynamics Simulation
TCM	Traditional Chinese Medicine
TEG	Triethylene Glycol
TMPRSS2	Transmembrane Serine Protease 2
Wi-A	Withaferin-A
Wi-N	Withanone